Available online at www.worldscientificnews.com

World Scientific News

An International Scientific Journal

WSN 196 (2024) 178-204 EISSN 2392-2192

Study of H-bonded dimer of organic linker-9,10-Antracenedicarboxylic acid: aided by computational DFT and Experimental FT-IR, FT-Raman, FT-NMR spectroscopy

Ramanna P. Kavali[1]*, Jayashree Tonannavar[2], J. R. Tonannavar[3], Sunanda Thakur[4]

[1]Department of Physics, Raichur University, Raichur-584133, Karnataka, India

[2]Department of Physics, Karnatak University, Dharwad-580003, Karnataka, India

[3]Department of Physics, Karnatak University, Dharwad-580003, Karnataka, India

[4]Department of Chemistry, GITAM School of Science, Gandhi Institute of Technology and Management, [Deemed to Be University], Hyderabad, 502 329, TS., India.

*Corresponding author: ramupknayak@gmail.com

ABSTRACT

A potential organic linker- 9,10-Anthracenedicarboxylic acid in Hydrogen bonded organic frameworks (HOFs) has been simulated –O─H•••O bonded dimer structure at B3LYP\6-311++G(d,p) level. The proposed dimer structure shows *local centre of inversion* confirmed by solid-phase IR and Raman spectra that exists in mutually exclusive bands. Experimental IR shows –O─H•••O characteristic signature medium intense bands are down/red-shifted ~ 450 cm^{-1}. Supported solution-phase ^1H NMR spectra recorded in d_6-DMSO solvent and –H•••O δ correlated to dimer structure. –O─H•••O bonded pentamer energies: Stabilization energy ($E^{(2)}$), Interaction energy (E_{HB}) and Binding energy are carried out by NBO, AIM and NCI analysis have provided a satisfactory electronic properties. And these are well consistent with structural and vibrational analysis.

(Received 18 July 2024; Accepted 15 August 2024; Date of Publication 16 September 2024)

Keywords: 9,10-Anthracenedicarboxylic acid, –O─H•••O bonded dimer, DFT, IR Raman and NMR.

1. INTRODUCTION

As a class, the anthracene fused carboxylic compounds and its derivatives are of interest as they contain a larger conjugating π-system – a precursor that enables the development of potential fluorescent materials [1-2]. Among these compounds, the anthracenedicarboxylic acids have been a subject of detailed discussions due to their powerful optoelectronic properties [1-5]. For instance, the photodimerization products of 9,10-anthracenedicarboxylic acid (ADA for short) have been used for treating tumors [6-7]. Among others, the greener applications of ADA include hydrogen storage,, methane storage and gas separation [1-5]. Therefore, in the recent past, detailed studies on the strategies and methods to prepare the anthracene fused dicarboxylic compounds have been undertaken due to their potential applications as discussed above. As ADA is a organic linker, it has been used as an intermediate in the design of porous materials [4-5]. In particular, a new type of zirconium metal-organic framework, UIO-66(H2ADC), has been synthesized by using ADA as a ligand [8]. It is noteworthy that the improved hydrogen uptake capacity of UIO-66(H2ADC) has been attributed to the improved hydrogen adsorption enthalpy of ADA due to the presence of a larger conjugating π-system in contrast to the smaller π-system of terephthalic acid. The synthesis and characterization of a series of anthracenecarboxylic acid derivatives in the solution and solid state is due to Lingyan Zhuet. *et al* [9]. The synthesis of metal-organic complexes having anthracene as a bulky backbone has been reported by Jun-Jie Wanget. *et al* [10]. Studies on the effect of the carbon backbone of benzene, naphthalene, and ADA on the luminescence properties of Eu-organic hybrid thin films are reported by Muhammad Safdaret *et al* [11]. The study suggests that the size of the organic backbone of the ligands is a crucial factor for tuning the luminescence properties of Eu-organic materials. The analysis of the photophysical properties of the compounds: 9,10-anthracenedicarboxylic acid, 1,4-anthracenedicarboxylic acid,and 2,6-anthracenedicarboxylic acid by employing steady-state absorption and emission spectroscopy and time-correlated single photon counting (TCSPC) emission lifetime spectroscopy technique has been reported by Jennifer M Rowe *et al* [12]. The authors point out that the addition of carboxylic groups to the anthracene ring perturbs the electronic transitions to varying degrees, causing substantial differences in the photophysical properties. Though ADA molecule, a organic linker, has many potential applications, its structural, vibrational, and electronic properties, including the structure of its H-bonded dimer, have not been investigated in detail. As a continuation of the studies on H-bonded organic linkers, we have systematically investigated the structural, vibrational, and electronic properties of the monomers and dimers of ADA.

The results of this combined experimental and computational investigation are presented herein Chapter five. The FT-IR spectrum of ADA has shown a broad and red-shifted band centered around 3000 cm^{-1} with maxima at 2896 and 2849 cm^{-1}. The bands are attributed to O─H stretch. These bands are absent in the FT-Raman spectrum. The vibrations of –C=O stretching have appeared as a local centro-symmetric IR active band at 1685 cm^{-1} and a Raman active band at 1632 cm^{-1}. These IR and Raman spectral features indicate that ADA exist as a O─H•••O bound species. To interpret the H-bond-induced vibrational spectra of ADA, we propose a dimer as a basic unit. Moreover, the appearances of local centro-symmetric bands in the experimental spectra suggest that the dimer is a cyclic-type. To compute the IR and Raman spectra of ADA dimer, as a first step, a conformational search was performed by a PES scan by rotating the two carboxylic groups at RHF/6-31G(d,p) level. This calculation followed by full geometry optimization and harmonic frequency analysis at DFT's B3LYP/6-311++G(d,p) level, yielded four stable monomers. In the next step, we computed a cyclic-dimer structure using two units of most stable monomer. The calculated vibrational spectrum of the dimer is in very good agreement with the experiment. The experimental bands due to O–H stretching at 2896 and 2849 cm^{-1} are calculated at 2873 and 2810 cm^{-1} respectively. Similarly, two mutually exclusive bands due to –C=O stretch observed at 1685 cm^{-1} (IR) and 1632 cm^{-1} (Raman) are computed at 1673 and 1652 cm^{-1} respectively. The NBO, AIM and NCI methods have been used to characterize the electronic and topological structure of the dimer. The results are consistent with the structural and vibrational analysis.

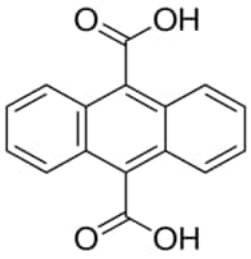

Figure 1. Molecular structure of 9,10-Anthracenedicarboxylic acid.

2. EXPERIMENTAL DETAILS

9,10 Antracenedicarboxylic acid (C_{16} H_{10} O_4; mp: >300 °C) supplied by Sigma-Aldrich Chemicals, Bengaluru, was used for IR, Raman, and NMR a spectral measurements. The IR spectra were record in the range 4000 – 400 cm^{-1} for 100 scans at spectral resolution of 2 cm^{-1} on a Nicolet-6700 FT-IR spectrometer equipped with an Alum standard ETC Ever-Glo radiation source, a KBr beam splitter, and DTGS detector.

The Raman spectra were measured in the range 4000 – 50 cm^{-1} with 500 scans at spectral resolutions of 2 cm^{-1} on a Bruker RFS27 stand-alone FT-Raman spectrometer module equipped with an Nd: YAG laser source operating at 1064 nm. The detection system included a liquid nitrogen cooled-Ge detector. The ^1H NMR spectra at room temperature were measured in d_6-DMSO on a *Jeol's* 400 MHz FT-NMR spectrometer with tetramethylsilane (TMS) as an internal reference.

3. COMPUTATIONAL DETAILS

We have performed structural, vibrational, and electronic properties for 9,10 Antracenedicarboxylic acid based on DFT method using *Gaussian 09 W, 16* and *Gauss View 5,6* suit of programs [13,14]. To reduce the computational cost, we first carried out a conformational search at RHF/6-31G(d,p) level at 300 k for a relaxed potential energy surface scan (PES) as a function of all the two –COOH groups, yielded a total of five potential energy minima points. The subsequent optimization and harmonic frequency analysis at B3LYP/6-311++G(d,p) level confirmed that all the five minima are true yielding a total of five monomers [15]. We label the five monomers as M_1, M_2, M_3, M_4 and M_5 (see Fig. 2). The estimated Boltzmann populations of all the monomers shows that the lowest energy monomer, M_1, shares 98 % of the total population. Fig. 3 presents the geometry-optimized molecular structure and numbering scheme for M_1. We constructed dimer structure bound by intermolecular O─H•••O bonds, using M_1 monomer. We next calculated harmonic frequencies for M_1 and dimer species, there were no imaginary frequencies. All the IR and Raman modes were computed potential energy distribution (PED) using VEDA program [16]. However, we selected dimer structure because it has provided consistent analysis of its results and excellent agreement with experiment. We have used gage independent atomic orbitals (GIAO) at B3LP/6-311++(d,p) level for the calculation of proton chemical shifts. We have also carried out stabilization energy ($E^{(2)}$), interaction energy (E_{HB}) of O─H•••O bonds by NBO and AIM analysis, respectively. We performed NCI calculations for the identification of H-bonds, *van der Waals,* and steric interactions in real space by isosurfaces using *Multiwavefunction* and VMD programs [17].

4. RESULT AND DISCUSSION

Fig. 1 shows the molecular structure for ADA. The molecular structure belongs to C_1 point group symmetry. Relaxed potential energy surface (PES) scan was carried out at RHF/6-31G(d,p) level by rotating the two torsional angles C7─C23─O25─H26 and C8─C27─O29─H30 with respect to the plane of the anthracene ring by a step size of 20º; nine global minima were found. The geometry optimization followed by the harmonic frequency analysis performed at RHF/6-31G(d,p) and B3LYP/6-311++G(d,p) level yielded four distinct stable conformers, i.e., monomers, say, M_1, M_2, M_3 and M_4 that are shown in Figure 2. Table 1 presents the energetics of all the monomer species. Out of four monomers, M_1 is found to be the most stable with the Boltzmann population of 95 %.

In the next step, we constructed O–H•••O bonded cyclic-dimer structure of ADA using only M_1 monomer as it is sharing 95 % of the total population. Figs. 3 and 4 presents the B3LYP/6-311++G(d,p) level geometry-optimized M_1 monomer and ADA's cyclic-dimer (hear after D_{11}) along with the numbering scheme used in the present study.

Table 1. Gibbs free energies, relative energies and Boltzmann populations of 9,10-Anthracenedicarboxylic acid.

Monomers	Gibbs Free Energy, G (hartree)	Relative Gibbs Free Energy, ΔG (hartree)	Relative Gibbs Free Energy, ΔG (kcal/mol)	Boltzmann Population (%)
M_1	–916.804110	0.00000	0.000	95.31
M_2	–916.799811	0.00429	2.692	2.08
M_3	–916.799806	0.00430	2.698	1.49
M_4	–916.799805	0.00431	2.699	1.35

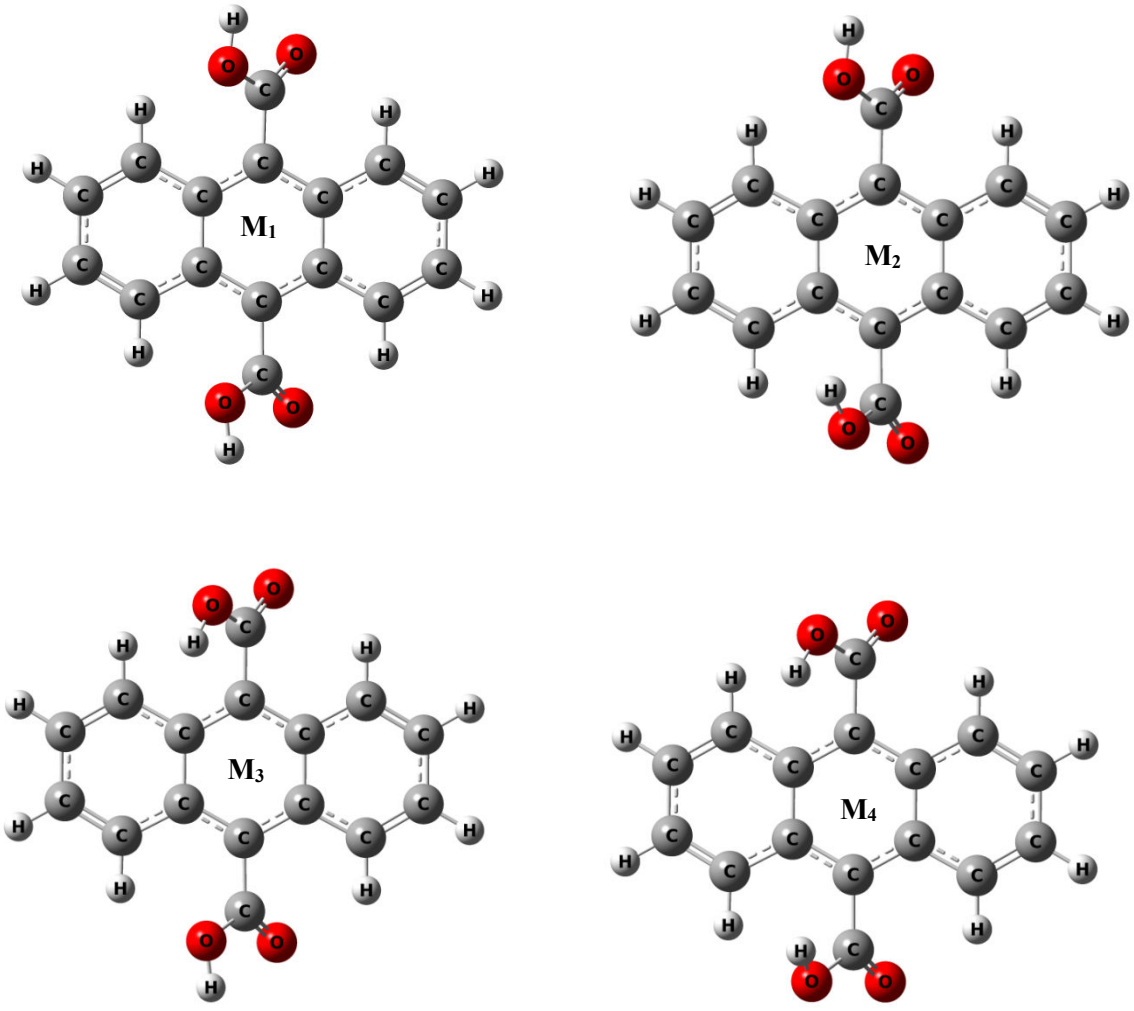

Figure 2. Distinct 4 structural conformers of 9,10-Anthracenedicarboxylic acid. Atom numbering is the same as Fig. 3.

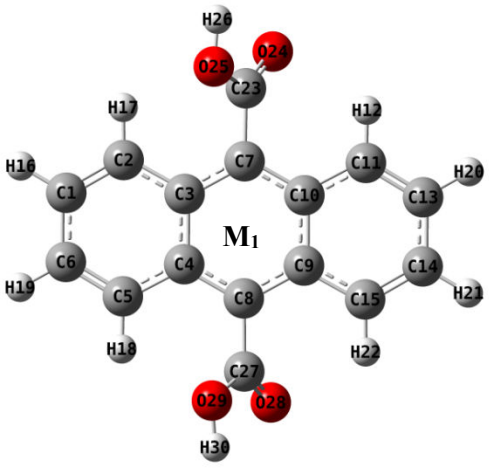

Figure 3. Optimized geometry of the M_1 monomer of 9,10-Anthracenedicarboxylic acid.

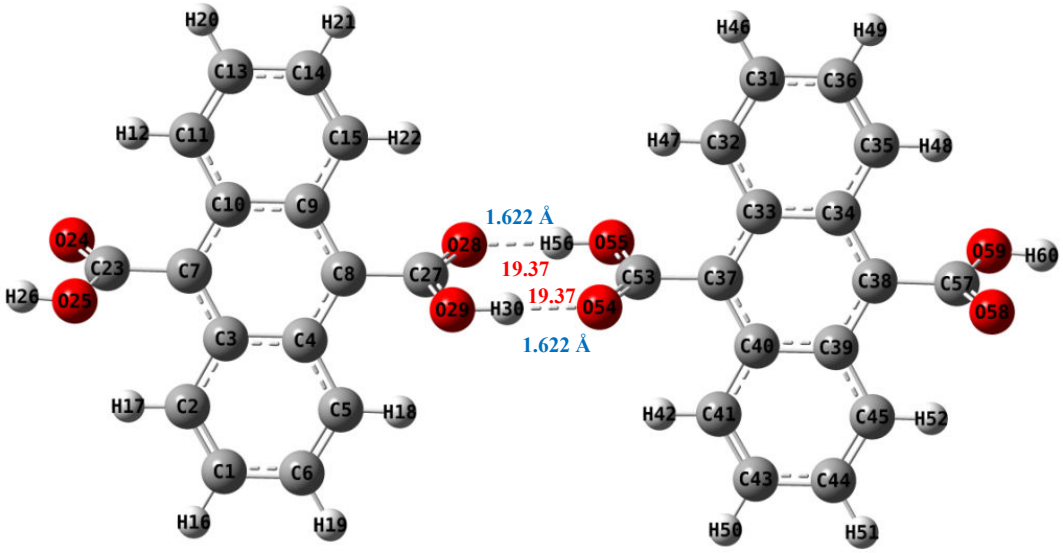

Figure 4. Optimized cyclic-dimer structure of 9,10-Anthracenedicarboxylic acid constructed using two units of the stable conformer M_1. Values of computed H-bond lengths H•••O (blue) and the corresponding stabilization energy (red, kcal/mol) that are also shown.

4.1. Structural characterization of the dimer

Since the single crystal XRD structural parameters of ADA molecule are not available in the literature, we have compared the calculated M_1 and D_{11} geometries with the nearest available structure of 9-Anthracenecarboxylic acid [13]. The crystal structure of 9-Anthracenecarboxylic acid has been reported by Lawrence J *et al.* [13].

The molecule crystallizes in the centrosymmetric space group $P2_1/n$. The anthracene ring is found to be almost planar due to the presence of strong conjugating π-system that provides a rigid planar structure. Furthermore, as a result of H-bonding between the carboxylic groups, 9-Anthracenecarboxylic acid exists as a cyclic-dimer with a local center of symmetry. Table 2 compares the optimized geometrical parameters of M_1 and D_{11} species with the SC-XRD data of 9-Anthracenecarboxylic acid. The crystal structure and DFT study on 9-Anthracenecarboxylic acid by Lingyan Zhu *et al* indicates that the molecule participates in the strong O–H•••O associations by forming head-to-tail and head-to-head O–H•••O bound dimer species [9]. Furthermore, owing to the steric factors in the gas phase, the head-to-tail structure is more stable than its head-to-head counterpart by approximately 12.66 cal/mole [9]. The calculated C–H bond lengths for ADA (see Table 2) at about 1.083 Å deviate from the experimental values by ~10 % on account of the low scattering factors of H atom [14]. The anthracene ring C–C bond lengths calculated in the range 1.365-1.443 Å are in better agreement with the experimental values of 1.357-1.432 Å with deviation of 0.01 Å. We note that the C–COOH bond lengths calculated at about 1.499 Å are in very good agreement with the reported value of 1.493 Å; with deviation of 0.007 Å. The bond lengths C27–O28 and C27–O29 measured at 1.240 and 1.292 Å are computed at 1.226 and 1.321 Å respectively. The covalent O–H bond length of 0.998 Å for D_{11} agree within 0.11 Å of the reported value. The large deviation has been again attributed to the difficulties in estimating the H atoms positions in the SC-XRD characterization of 9-Anthracenecarboxylic acid [13]. The anthracene C–C–C angles in Table 2 differ by less than 1 %. For 9-Anthracene carboxylic acid crystal, the O•••H bond length and O–H•••O bond angles are measured at 1.540 Å and 176.0° respectively. These values substantiates that the H-bonds are rather strong and almost linear. The corresponding bond-lengths and angles calculated for D_{11} at 1.622 Å and 176.8° are in very good agreement with the experiment. Furthermore, the calculated O•••H bond distance of 1.662 Å being less than the sum of the *van der Walls* radii of O and H atoms (2.72 Å) satisfy the geometrical criteria for the existence of H-bond between the two carboxylic groups. The O–H•••O bond lengths and bond angles shown in the Table 2 confirm that the H-bonds in ADA are strong [15].

Table 2. Geometrical parameters and hydrogen bonding geometry of 9,10-Anthracenedicarboxylic acid. (* 9-anthracene carboxylic acid)

Bond lengths (Å)	***X-ray**	**M_1**	**Dimer**	**Δ %**
C1-C2	1.357	1.365	1.365	0.58
C1-C6	1.411	1.420	1.420	0.63
C1-H16	0.980	1.083	1.083	10.5
C2-C3	1.432	1.431	1.431	0.06
C2-H17	0.980	1.081	1.081	10.3
C3-C4	1.431	1.443	1.443	0.83
C3-C7	1.412	1.407	1.407	0.35
C4-C5	1.432	1.431	1.431	0.06
C4-C8	1.412	1.407	1.408	0.35
C5-C6	1.357	1.365	1.365	0.58
C5-H18	0.980	1.081	1.080	10.3
C6-H19	0.980	1.083	1.083	10.5
C7-C10	1.411	1.408	1.408	0.21
C7-C23	1.493	1.500	1.500	0.46
C8-C9	1.411	1.408	1.409	0.20
C8-C27	1.493	1.500	1.499	0.45
C9-C10	1.431	1.443	1.443	0.83
C9-C15	1.432	1.431	1.431	0.06
C10-C11	1.432	1.431	1.431	0.06
C11-H12	0.980	1.081	1.081	10.3
C11-C13	1.357	1.365	1.365	0.58
C13-C14	1.411	1.420	1.420	0.63
C13-H20	0.980	1.083	1.083	10.5
C14-C15	1.357	1.365	1.365	0.58
C14-H21	0.980	1.083	1.084	10.5
C15-H22	0.980	1.081	1.080	10.3
C23-O24	-	1.206	1.206	-
C23-O25	-	1.356	1.355	-
O25-H26	-	0.970	0.970	-
C27-O28	1.240	1.206	1.226	1.12
C27-O29	1.292	1.356	1.321	2.24
O29-H30	1.110	0.970	0.998	10.0
Bond angles (°)				
C2-C1-C6	120.2	120.3	120.3	0.08
C2-C1-H16	-	119.9	119.9	-
C6-C1-H16	-	119.7	119.7	-
C1-C2-C3	121.1	121.3	121.3	0.01
C1-C2-H17	-	119.4	119.5	-
C3-C2-H17	-	119.2	119.1	-
C2-C3-C4	119.2	118.3	118.3	0.75
C2-C3-C7	121.5	122.4	122.3	0.65
C4-C3-C7	119.3	119.2	119.2	0.08
C3-C4-C5	117.4	118.3	118.1	0.59
C3-C4-C8	118.8	119.2	119.1	0.25
C5-C4-C8	121.5	122.4	122.6	0.74
C4-C5-C6	121.1	121.3	121.3	0.16
C4-C5-H18	-	119.1	119.2	-
C6-C5-H18	-	119.4	119.4	-
C1-C6-C5	121.0	120.3	120.4	0.49
C1-C6-H19	-	119.6	119.6	-
C5-C6-H19	-	119.9	119.8	-

C3-C7-C10	121.5	121.5	121.6	0.08
C3-C7-C23	119.0	119.9	119.9	0.75
C10-C7-C23	119.5	118.4	118.4	0.92
C4-C8-C9	121.5	121.5	121.5	0.00
C4-C8-C27	119.0	119.9	119.7	0.58
C9-C8-C27	119.5	118.4	118.7	0.66
C8-C9-C10	118.8	119.1	119.2	0.33
C8-C9-C15	121.7	122.4	122.5	0.57
C10-C9-C15	117.5	118.3	118.2	0.59
C7-C10-C9	119.5	119.1	119.1	0.33
C7-C10-C11	121.7	122.4	122.3	0.49
C9-C10-C11	118.8	118.3	118.4	0.33
C10-C11-H12	-	119.1	119.1	-
C10-C11-C13	121.3	121.1	121.1	0.16
H12-C11-C13	-	119.6	119.6	-
C11-C13-C14	120.0	120.4	120.3	0.25
C11-C13-H20	-	119.8	119.9	-
C14-C13-H20	-	119.6	119.7	-
C13-C14-C15	121.3	120.4	120.4	0.74
C13-C14-H21	-	119.6	119.6	-
C15-C14-H21	-	119.8	119.8	-
C9-C15-C14	121.0	121.1	121.2	0.16
C9-C15-H22	-	119.1	119.1	-
C14-C15-H22	-	119.6	119.5	-
C7-C23-O24	-	125.4	125.3	-
C7-C23-O25	-	112.4	112.4	-
O24-C23-O25	-	122.1	122.1	-
C23-O25-H26	-	106.8	106.9	-
C8-C27-O28	121.4	125.4	122.5	0.90
C8-C27-O29	116.2	112.4	114.1	1.80
O28-C27-O29	122.4	122.1	123.2	0.65
C27-O29-H30	-	106.8	110.0	-

H-bonds	**O ─ H (Å)**	**H · · · O (Å)**	**O ─ O (Å)**	**O ─ H · · ·O (°)**
O55 ─ H56 · · · O28	1.013	1.622	2.635	176.8
O29 ─ H30 · · · O54	1.013	1.622	2.635	181.3
Expt. O ─ H · · · O	1.110	1.540	2.646	176.0

Note: Δ % refer to deviations between experimental and dimer values.

4.2. Vibrational analysis of dimer modes

The ADA molecule monomer, M_1, consisting of 30 atoms has 84 normal modes of vibrations while the dimer, D_{11}, composed of two M_1 structures has 174 modes including 6 modes due to H-bonds. The M_1 and D_{11} structures belong to C_1 point group symmetry, all the normal modes of vibrations are IR and Raman active. The observed and computed IR and Raman spectra are shown in Fig. 5.4 and 5.5 respectively.

The complete vibrational assignments of the modes aided by potential energy distribution (PED) along with the intensities are summarized in Table 5.3. The calculated harmonic frequencies presented in the Table 5.2 are scaled with the scaling factors 0.983 up to 1700 cm^{-1} and 0.958 for greater than 1700 cm^{-1} [16]. In the M_1 and D_{11} species, the carbon-hydrogen stretching vibrations are observed in the range 3000-3100 cm^{-1} [17-19]. As seen from the Table 5.3, out of eight monomeric C─H stretching modes (υ_3-υ_{10}) calculated at 3078, 3076, 3076, 3074, 3051, 3051, 3037 and 3037cm^{-1}, a total of six bands are observed with medium to weak intensity IR bands at 3096, 3061, 2999, 2953 cm^{-1} and strong to weak intensity Raman bands at 3087, 3039, 2997 cm^{-1}. All these bands are due to pure C─H stretching vibrations. Surprisingly, upon dimerization, some of the C─H stretch show small blue-shifts. The experimental and computed C─H stretching frequencies differ by 0.09-2.9 % deviation. Generally, the C─H in-plane and out-of-plane bending vibrations appear in the 1000-1300 cm^{-1} and 750-1000 cm^{-1} regions respectively [20,21]. The IR absorptions due to C─H in-plane bending are observed as a very strong band at 1256 cm^{-1}, strong at 1298 cm^{-1}, medium bands at 1174, 1170 cm^{-1} and weak band at 1277 cm^{-1}. The bands are computed to be very strong to very weak at 1263, 1311, 1199, 1192 and 1277 cm^{-1}. The medium and weak intensity Raman bands observed at 1292 cm^{-1} and 1232 cm^{-1} are computed at 1283 and 1226 cm^{-1} respectively. The C─H out-of-plane bending modes observed in IR as very strong band at 787 cm^{-1}, strong at 924 cm^{-1}, medium at 994 cm^{-1} and weak band at 832 cm^{-1} are computed at 779, 909, 993 and 838 cm^{-1} respectively. The corresponding Raman bands are observed to be weak at 993 and 944 cm^{-1}.

The accurate assignments of the modes due to the ring C─C and C=C stretching is important as they are highly characteristic of the anthracene itself. The modes are normally observed in the 1650-1400 cm^{-1} region [22]. Varsanyi has assigned the bands in the 1625-1590, 1590-1575, 1540-1470, 1465-1430 and 1380-1280 cm^{-1} region to aromatic-ring C─C stretching vibrations [19]. In the Fig. 5.4, the IR bands at 1566, 1548, 1530 1452, 1422, 1359 and 1277 cm^{-1} are identified as C─C stretching vibrations. The bands are computed at 1569, 1544, 1542, 1473, 1420, 1360 and 1277 cm^{-1} respectively. The strong and medium intensity Raman lines at 1561 and 1292 cm^{-1} are calculated at 1569 and 1283 cm^{-1} respectively. We note that, there is a close agreement between the experimental and computed vibrational frequencies as the deviation is less than 1 %. The very strong to weak intensity IR absorptions at 924, 832 and 787 cm^{-1} are assigned to C─C─C in-plane bending and they are calculated at 909, 838 and 779 cm^{-1} respectively. Out-of-plane C─C─C bends calculated at 668, 638, 581, 471 and 405 cm^{-1} are assigned to the 674, 640, 588, 465 and 409 cm^{-1} bands. These assignments are in line with M. Karbacak values [23]. Upon comparison of the Raman spectrum of the ADA with that of benzene, a strong Raman line expected in the 910-1000 cm^{-1} attributed to aromatic ring breathing has been observed as weak band at 993 cm^{-1} due to the loss of the rigidity in the ADA molecule [24]

As discussed in the Introduction section, the IR and Raman spectra clearly show that each monomeric unit of ADA is strongly bound by four O─H•••O inter-molecular H-bonds. This bonding is mediated by the interaction of two -COOH groups. Thus, the bands due to –C=O and O─H stretching are red-shifted (Fig. 5.4 and 5.5). The broad and medium intensity absorption in the 2500-3100 cm^{-1} region with several maxima has been readily assigned to the absorption due to O─H stretch. The O–H stretching bands are observed to be at 2896, 2849 cm^{-1}. These absorptions are calculated fairly accurately at 2873, 2810 cm^{-1} with 99.92 % of PED contributions. As opposed to the red-shifts in stretching frequencies, the OH in-plane and out-of-plane bending vibrations have shown blue-shifts. Many IR bands measured at 1452, 1422, 1298 and 1232 cm^{-1} due to OH in-plane bindings are computed at 1448, 1418, 1311 and 1233 cm^{-1} respectively. The C=O stretching modes of ADA are observed to be stronger than the ketonic C=O stretching that normally appears in the region 1640-1700 cm^{-1} [22]. A very strong IR at 1685 cm^{-1} and medium Raman at 1632 cm^{-1} have been readily assigned to C=O stretching vibrations. These bands are computed at 1673 and 1652 cm^{-1} respectively. The presence of IR absorption at 1685 cm^{-1} with the absence of a corresponding Raman line and the presence of Raman at 1632 $cm^{-1}$with the absence of a corresponding IR suggest that the C=O stretching modes are mutually exclusive, indicating the existence of a local center of inversion symmetry in the cyclic-dimer structure. The C─O stretching modes have appeared as strong bands in the region 1450-1200 cm^{-1} [25,26]. It is well known that the Raman is more sensitive to bands due to O•••H bonds in the lower wavenumber region. However, the accurate assignments are complicated by the presence of lattice modes. Thus, the comparison of the calculated frequencies with the experiment proves to be very useful. A strong Raman line calculated at 84 cm^{-1} assigned to O•••H stretching has been observed at 84 cm^{-1}.

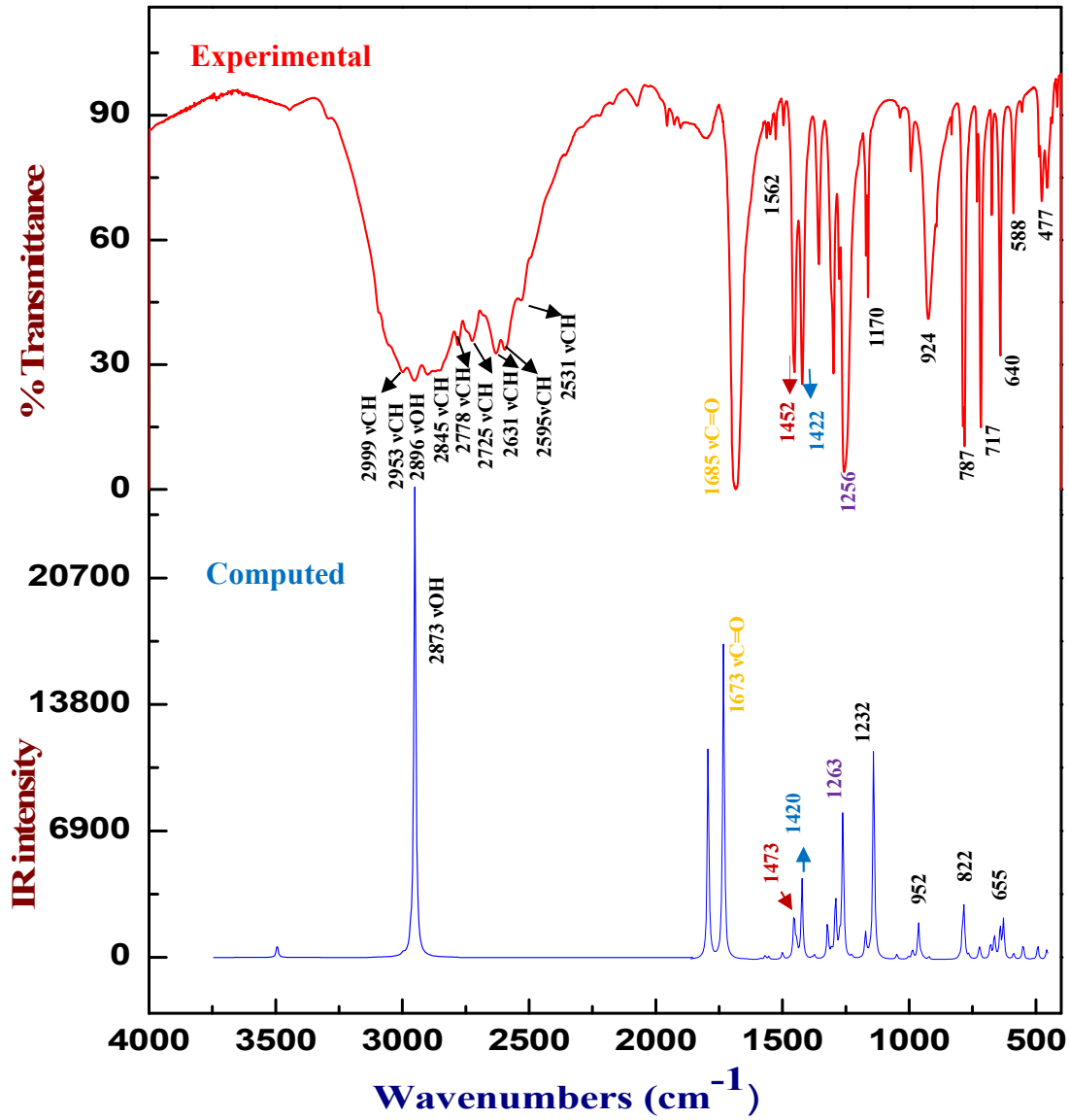

Figure 5. Observed IR spectrum compared with computed dimer spectrum of 9,10-Anthracenedicarboxylic acid. In the experimental IR spectra in the region 2500-3100 cm^{-1} the bands due to C─H and H-bonded O─H modes are too close to be seen distinct. The same color bands marked with frequencies in both spectra correspond to one another, showing good agreement. The C=O band at 1685 cm^{-1} arises in O─H•••O bond, corresponding to the Raman band at 1632 cm^{-1} and both are mutually exclusive of their occurrence for reasons discussed in the text.

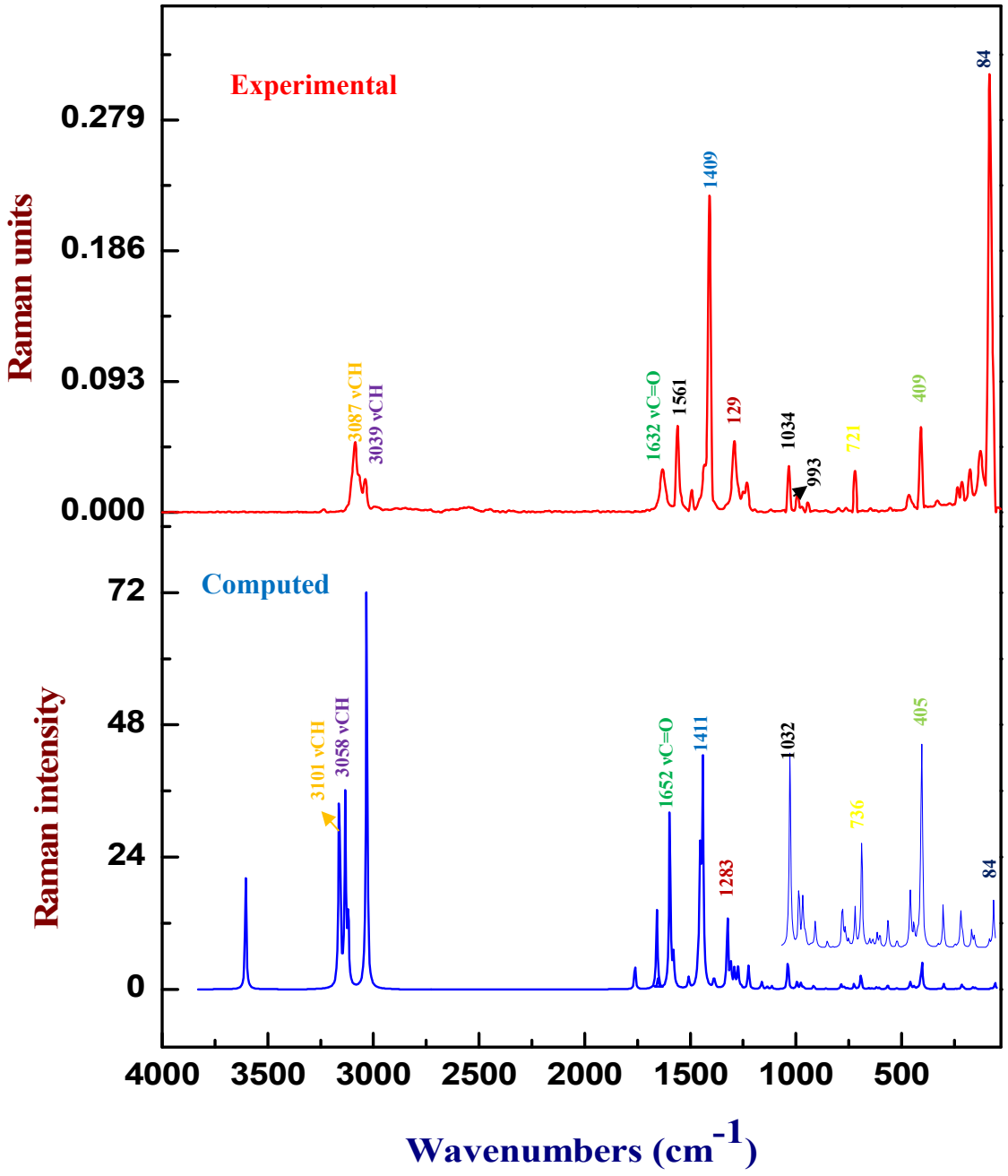

Figure 6. Observed Raman spectrum compared with simulated dimer spectrum of 9,10-Anthracenedicarboxylic acid. Here the bands due to C─H modes distinctly appear at 3087, 3039 cm^{-1}. The same color bands marked with frequencies in both spectra correspond to one another, showing good agreement. The C=O band at 1632 cm^{-1} arises in O─H•••O bond corresponding to the IR band at 1685 cm^{-1}; both are mutually exclusive of their occurrence. A very strong band at 84 cm^{-1} corresponds to 84 cm^{-1} band of dimer.

Table 3. Comparison of experimental vibrational frequencies (cm^{-1}) with computed monomer and dimer values with intensities, percentage deviations, and vibrational assignments for 9,10-Anthracenecarboxylic acid.

Normal modes	Experimental		Computed		Intensity[b]		Δ %	Vibrational Assignments [PED %] [c]
	IR	Raman	M_1	Dimer[a]	I_{IR}	I_{Ra}		
ν_1	3447w	-	3581	3473	36.9	415.9	0.75	OH ν_s [97]
ν_2	3293	-	3581	3473	76.7	199.9		OH ν_{as} [97]
ν_3	-	-	3078	3110,3110	10.4	155.5	-	CH ν [88]
ν_4	-	-	3076	3107,3107	6.9	137.1	-	CH ν [92]
ν_5	3096w	-	3076	3105,3105	6.4	67.3	0.29	CH ν [90]
ν_6	-	3087s	3074	3101,3101	4.5	67.4	0.42	CH ν [93]
ν_7	3061w		3051	3058,3058	0.01	998.0	0.09	CH ν [64]
ν_8	-	3039 m	3051	3058,3058	0.01	0.009	0.62	CH ν [72]
ν_9	2999m	2997w	3037	3041,3041	2.4	295.6	1.40	CH ν [72]
ν_{10}	2953m	-	3037	3041,3041	44.4	0.005	2.18	CH ν [85]
ν_{11}	2896m	-	-	2873	7033.8	0.001	0.79	OH ν_{as} H-bond [99]
ν_{12}	2849w	-	-	2810	0.003	1977.2	1.36	OH ν_s H-bond [92]
ν_{13}	2778m	-	-	-	-	-	-	1422+1357
ν_{14}	2725m	-	-	-	-	-	-	1422+1298
ν_{15}	2631m	-	-	-	-	-	-	1457+1174
ν_{16}	2596m	-	-	-	-	-	-	1298+1298
ν_{17}	2528w	-		-	-	-	-	1357+1170
ν_{18}	-	-	1718	1687	68.5	213.9	-	C=O ν_s [77]
ν_{19}	-	-	1713	1687	480.6	30.5	-	C=O ν_{as} [77]
ν_{20}	1685vs	-	1642	1673	979.7	0.00	0.65	C=O ν_s [70]
ν_{21}	-	1632m	1627	1652	0.00	870.0	1.22	C=O ν_{as} [67]
ν_{22}	1566w	1561s	1570	1570,1569	5.4	495.4	0.20	CC ν [48]
ν_{23}	1548w	-	1551	1544,1544	26.7	0.1	0.25	CC ν [46]
ν_{24}	1530w	-	1537	1542,1542	90.4	0.009	0.78	CC ν_s [12], COH δ_{sci} [28], HCC δ_{roc} [20]
ν_{25}	1495w	1494w	1500	1518,1517	15.3	121.8	1.47	HCC δ_{roc} [32], HCC δ_{sci} [26]
ν_{26}	-	-	1458	1482,1480	68.8	3.9	-	CO ν [12], COH δ [24], HCC δ [30]
ν_{27}	1452s	-	1454	1473,1473	73.8	0.3	1.44	CC ν [14], CCH δ [33]
ν_{28}	-	-	1416	1443	207.0	0	-	OC ν [10], COH δ_{roc} [29], CCH δ [18]
ν_{29}	-	-	1392	1432	0	141.4	-	CO ν [13], COH δ_{sci} [28], CCH δ [23]
ν_{30}	1422s	-	1381	1420,1418	28.9	732.0	0.14	HCC δ [30], CC ν [14]
ν_{31}	-	1409vs	1358	1411,1413	38.4	253.7	0.14	HCC δ [32], COH δ [24]
ν_{32}	-	-	1319	1372,1372	80.11	46.4	-	CCC δ_{sci} [23], CC ν_s [20], COH δ [34]
ν_{33}	1359s	-	1303	1360,1360	24.9	22.6	0.07	CC ν [22], COH δ [14], HCC δ [10]
ν_{34}	-	-	1280	1324,1324	3.5	32.2	-	HCC δ_{roc} [32], CCC δ [12]
ν_{35}	1298s	-	1277	1312,1311	55.0	411.9	1.00	HCC δ_{roc} [22], CCC δ [10], COH δ [28]

Cont…

ν_{36}	-	1292m	1268	1283,1283	10	14.9	0.69	CC ν [17], HCC δ_{roc} [32]
ν_{37}	1277w	-	-	1277,1277	55.5	677.2	0	HCC δ [12], CC ν [23]
ν_{38}	1256vs	-	-	1263,1263	9.4	76.3	0.55	CCC δ [20], HCC δ [27]
ν_{39}	-	1232w	1236	1233,1226	585.1	93.9	0.07	CO ν [18], HCC δ [20], COH δ [28]
ν_{40}	-	-	1186	1216,1216	0.6	3.4	-	HCC δ_{sci} [28], HCC δ_{roc} [26]
ν_{41}	1174m	-	1184	1199,1199	34.5	15.7	2.12	HCC δ_{roc} [11], HCC δ_{sci} [11]
ν_{42}	1170m	-	1168	1193,1192	77.0	10.5	1.88	HCC δ [26], COH δ [18]
ν_{43}	-	-	1147	1124,1124	1.3	1.8	-	CCC δ [14], HCC δ [33]
ν_{44}	-	-	1124	1098,1096	873.2	39.1	-	OC ν [26], HOC δ [29]
ν_{45}	-	-	1115	1052,1051	8.1	1.4	-	CC ν [23], CCH δ [21], CC ν [26]
ν_{46}	-	-	1038	1042,1042	2.5	90.8	-	CC ν [12], CCC δ [13], CCH δ [18]
ν_{47}	1036w	1034m	1031	1032	195.8	0	0.19	CCOH γ_w [15], COHO γ_w [15]
ν_{48}	-	-	979	1018,1017	5.4	4.6	-	HCCC γ_{tw} [50], CCCC γ_{tw} [10]
ν_{49}	-	-	978	1015,1015	1.6	2.9	-	HCCC γ_{tw} [13], HCCC γ_{tw} [12]
ν_{50}	-	-	974	998	0	8.5	-	HOCC γ_{tw} [24], OHOC γ_{tw} [14]
ν_{51}	994m	993w	964	993,992	7.6	9.3	0	HCCC γ_{tw} [22], HCCC γ_w [24]
ν_{52}	-	-	960	990,990	1.5	2.3	-	HCCC γ_{tw} [24], HCCC γ_w [23]
ν_{53}	-	-	955	989	40.6	0	-	CCCC γ_{tw} [28], CCC δ [16]
ν_{54}	-	-	942	984	0	18.5	-	CCCC γ_w [10], CCOH γ_{tw} [24], HCCC γ_{tw} [22]
ν_{55}	-	-	896	962,961	16.5	13.9	-	CCC δ [33], CCCC γ_{tw} [27]
ν_{56}	-	944w	845	953,909	80.7	17.2	0.84	HCCC γ_{tw} [39], CCCC τ [18], CO ν [12]
ν_{57}	924s	-	840	952,909	5.5	2.9	1.62	HCCC γ_w [82]
ν_{58}	-	-	793	894,893	28.3	0	-	CC ν_s [23], CC ν_{as} [23], CCC δ [14]
ν_{59}	-	-	781	879,879	1.02	0.2	-	HCCC γ_{tw} [12], CCOH γ_{tw} [10]
ν_{60}	832w	-	760	839,838	4.7	16.2	0.72	CCCC γ_w [10], CCCC τ [12], HCCC γ_{tw} [12]
ν_{61}	-	-	752	822,821	106.9	0.6	-	HCCC γ_{tw} [27], HOCC γ_{tw} [29]
ν_{62}	787vs	-	740	779,778	0.1	7.9	1.01	CCCC γ_{tw} [21], HCCC γ_w [12]
ν_{63}	-	-	730	766,766	1.9	0.3	-	OCOC τ [32], CCCH γ_{tw} [13]
ν_{64}	-	-	727	762,757	91.7	3.6	-	CCCC γ_{tw} [13], CCCC τ [31]

Cont…

ν_{65}	-	-	683	756,753	25.9	1.6	-	OCOC γ_{tw} [18], CCCC τ [21]
ν_{66}	-	721m	659	736,736	90.1	0.2	2.08	HOCC γ_{w} [22] OCOC γ_{tw} [16]
ν_{67}	717vs	-	648	698,693	8.0	36.0	2.64	OCO δ_{sci} [26], OCOC γ_{tw} [26]
ν_{68}	674w	-	630	668	32.2	0	0.89	CCCC τ [32], OCO δ_{sci} [24]
ν_{69}	-	-	629	664,663	57.8	2.0	-	HOCC γ_{tw} [22], CCCC γ_{tw} [18]
ν_{70}	-	-	625	655,655	148.4	5.7	-	OCOC γ_{tw} [22], CCCC γ_{tw} [18]
ν_{71}	-	-	620	655	0.1	2.4	-	CCC δ_{sci} [17], COCO γ_{tw} [16]
ν_{72}	640s	-	558	638,638	129.5	0	0.31	HOCC γ_{tw} [44], CCC δ_{sci} [17], CCCC γ_{w} [18]
ν_{73}	-	-	533	625,625	89.0	9.8	-	CCCC τ [21], HOCC γ_{tw} [22]
ν_{74}	588m	-	487	581,579	6.1	7.7	1.19	CCCC γ_{tw} [36], CCCC γ_{tw} [21], CCCC τ [12]
ν_{75}	-	-	466	554,551	28.9	3.4	-	HOCC γ_{tw} [30], CCCC τ [18]
ν_{76}	-	-	457	510,510	3.8	0.6	-	HCCC γ_{tw} [16], CCCC τ [20]
ν_{77}	-	-	429	486,486	0.6	29.1	-	CCCC γ_{tw} [29], HCCC γ_{tw} [16]
ν_{78}	477m	465w	427	471,459	96.2	19.0	1.25	CCC δ_{sci} [10], OHO δ_{sci} [22], HOCC γ_{tw} [16]
ν_{79}	456m	-	410	446,445	9.6	22.8	2.19	CCCC τ [21], OH ν [15], OHOC γ_{w} [16]
ν_{80}	-	-	399	441,433	13.4	1.9	-	HCCC τ [20], HOCO γ_{w} [16]
ν_{81}	415w	-	321	417,415	8.7	11.2	0	CCCC γ_{tw} [27], HOCO τ [21]
ν_{82}	-	409m	269	405,405	1.0	65.6	0.97	CCCC τ [27]
ν_{83}	-	-	236	373,348	60.0	0.4	-	OHOC δ_{roc} [30], CCCC τ [23]
ν_{84}	-	-	230	318,289	34.0	15.8	-	COCO γ_{tw} [23], CCCC τ [20]
ν_{85}	-	-	227	277,273	1.9	1.9	-	CCCC γ_{tw} [25], CCCC γ_{w} [20], COHO γ_{w} [20]
ν_{86}	-	235w	101	234,217	4.8	8.3	0.42	HOCO γ_{tw} [21], CCCC τ [24], HCCC τ [17]
ν_{87}	-	215w	100	197,196	1.4	4.5	8.3	HOCO γ_{tw} [22], CCOH γ_{tw} [30]
ν_{88}	-	176m	98	153,141	11.0	3.3	13.0	OHCO γ_{w} [30], CCCC τ [40], OHCO γ_{tw} [30]
ν_{89}	-	127m	56	107,105	0.6	2.7	19.4	HCCC γ_{w} [88]
ν_{90}	-	-	41	103,103	4.8	1.0	-	CCCC γ_{w} [46], HCCC τ [40]
ν_{91}	-	84vs	37	97,84	1.2	15.1	0	OCOH γ_{tw} [62], HCCC τ [30]

Note: Intensities: vs = very strong, s = strong, m = medium, w = weak, vw = very weak, sh = shoulder. Mode description: ν_s = symmetric stretching, ν_{as} = asymmetric stretching, δ_{sci} = scissoring, δ_{roc} = rocking, γ_w = wagging, γ_{tw} = twisting, τ = torsional. [a] Double bands values refer to correspondingly similar bonds. [b] = Computed IR intensity (I_{IR}) in KM/Mole, Raman intensity (I_{Ra}) in A^4/AMU. [c] = PED contribution (in %) given in square bracket. Δ % refers to deviations calculated w.r.t. dimer & experimental values.

4.3. NMR structural analysis

The NMR analysis is one of the most efficient techniques that has been routinely used to characterize the molecular structure in terms of chemical shifts (δ) measured with respect to an internal standard. The experimental and B3LYP/6-311++G(d,p) level calculated ^{1}H NMR spectra of ADA in *d_6*-DMSO solvent are shown in the Fig. 6 and 7 respectively. The theoretical δ values are calculated by using gauge independent atomic orbital's (GIAO) method. Table 3 compares the experimental and calculated δ values. In D_{11} (see Fig. 4), we find seven types of magnetically different protons. Accordingly, seven peaks are expected in the ^{1}H NMR spectrum. Surprisingly, the solute-solvent interactions have not affected the resonances of carboxylic protons. The signal observed at 14.19 ppm is assigned to the resonances of the protons of H-bonded carboxylic groups (H30, H56). The corresponding δ has been computed at 14.4 ppm. The non-H-bonded protons of carboxylic groups (H26, H60) resonances have not appeared in the experimental spectrum but are predicted at ~6.7 ppm. The anthracene ring proton resonances (H16, H19, H20 and H21) appeared in the 7-8 ppm region. The NMR signals due to anthracene ring protons (H48, H52) that are in the close proximity of carboxylic groups have appeared at 8.04 ppm. The signals are calculated at 8.6 ppm.

Table 4. Observed and dimer computed chemical shifts (δ) of 9,10Anthracenedicarboxylic acid.

Protons	**Exp.**	**dimer (δ)**	**$\delta^*_{TMS} - \delta_c$**
H16, H19, H20, H21	7.66	39.7	7.9
	-	39.6	7.8
H48, H52	8.04	40.4	8.6
H12, H17	-	40.3	8.5
H22, H18, H47, H42	-	40.6	8.8
H30, H56	14.19	46.2	14.4
H26, H60	-	38.5	6.7

Note: δ^*_{TMS} = 31.3 ppm. Ref: † [8]

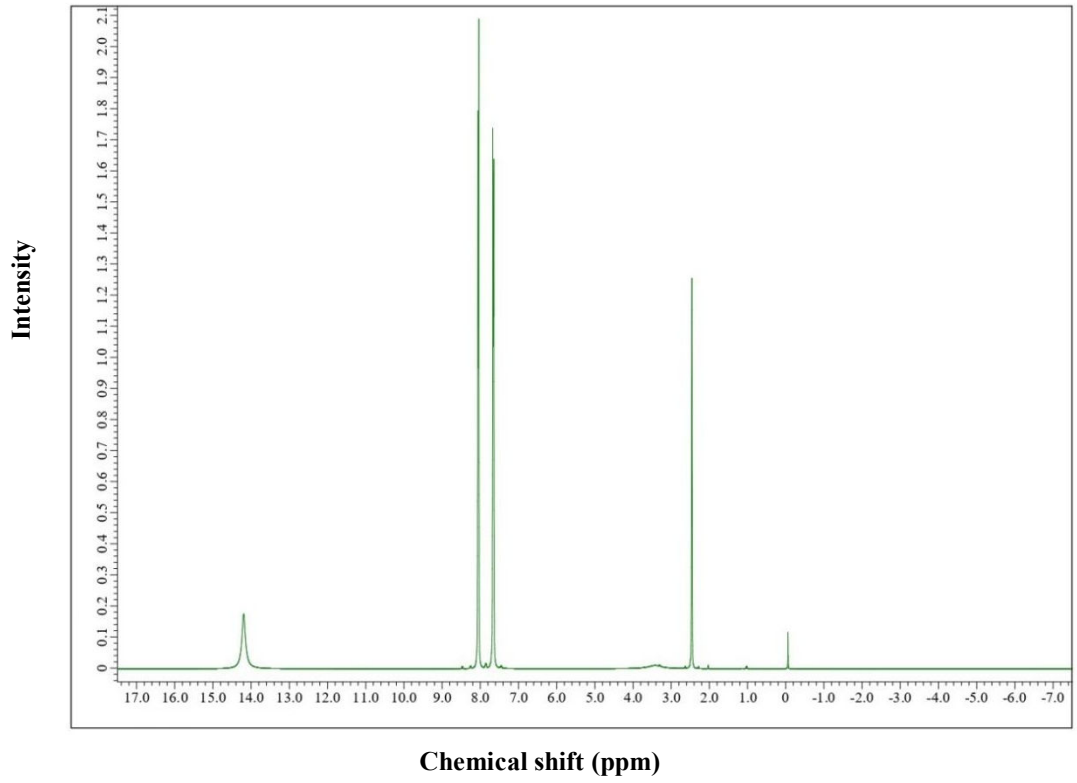

Figure 7. The experimental ^{1}H NMR spectrum of 9,10-Anthracenedicarboxylic acid recorded in d_6-DMSO solvent. The O─H•••O bonding δ observed at ~ 14 ppm.

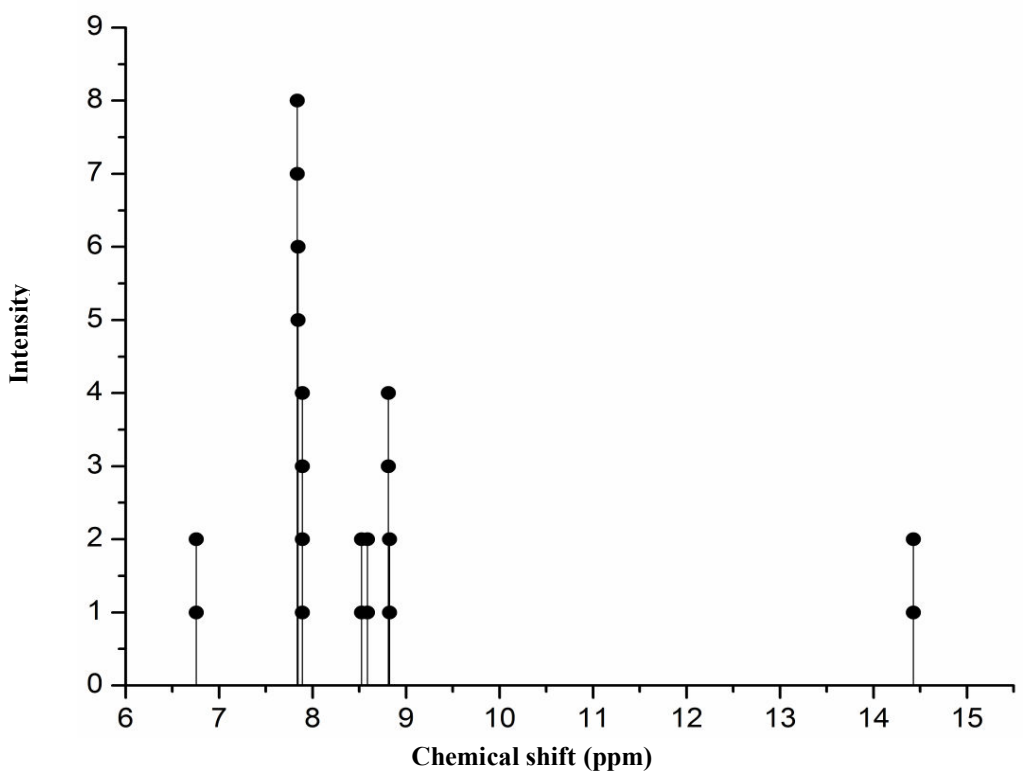

Figure 8. Computed ^{1}H NMR spectrum in DMSO solvent for the cyclic-dimer of 9,10-Anthracenedicarboxylic acid.

4.4. NBO analysis

To analyze the electronic charge distribution on the H-bond bridging atoms and charge transfer from donor orbital, n(O), to acceptor anti-bonding orbital, σ^*(O─H), in the n(O)→σ^*(O─H) hyperconjugation, we have used NBO method. Natural atomic charges, stabilization energies, orbital occupancies, polarization coefficients, NBO description, and contribution of s character for D_{11} are summarized in the Table 5, 6 and 7. Fig. 5a and 5b present orbital overlaps in D_{11}. As can be seen from the Table 5.5, upon dimerization, electronic charge on the bridging atoms is delocalized. The non-bonded H atoms of carboxylic groups (H26, H60) have 0.47829 au atomic charges. Similarly, the ketonic oxygen and hydroxyl oxygen atoms (O24, O58 and O25, O59) show −0.57942 and −0.68221 au charges. Upon dimerization, the bonded H atoms of carboxylic groups (H30, H56) have become slightly more positive due to n(O)→σ^*(O─H) hyperconjugation and the charges are calculated at 0.50596 au Consequently, the bridging oxygen atoms, O28 and O54, have become slightly more negative (−0.65825 au) as compared to O24, O58 atoms –ve atomic charges (−0.57942 au). The substantial orbitals overlap of n(O) and σ^*(O─H) in D_{11} as shown graphically in the Fig. 5.8 confirmed the presence of two strong O─H•••O bonds between the -COOH groups. The net charge transfer due to n(O28) →σ^*(O55─H56) and n(O54)→σ^*(O29─H30) hyperconjugations has stabilized the D_{11} structure by 77.21 kcal/mol. We note that both the hyperconjugations are equal in strength as the stabilization energies are equal (38.47 kcal/mol, see Table 5). Consequently, the absorptions due to O55─H56 and O29−H30 stretch are almost equally red-shifted (2896 and 2849 cm^{-1} respectively, see Fig. 4). The –COOH groups are involved in H-bonds those orbital occupancies of σ components, polarization coefficient, NBO description and contribution s characters are listed in Table 6.

Table 5. Atomic natural charges for dimer of 9,10-Anthracenedicarboxylic acid.

Atoms	Natural Charge (au)	Natural Population Total	Atoms	Natural Charge (au)	Natural Population Total
C1	–0.18547	6.18547	C31	–0.18458	6.18458
C2	–0.17415	6.17415	C32	–0.17487	6.17487
C3	–0.03052	6.03052	C33	–0.02753	6.02753
C4	–0.02753	6.02753	C34	–0.03053	6.03053
C5	–0.17487	6.17487	C35	–0.17414	6.17414
C6	–0.18458	6.18458	C36	–0.18547	6.18547
C7	–0.08749	6.08749	C37	–0.08579	6.08579
C8	–0.08579	6.08579	C38	–0.08749	6.08749
C9	–0.02577	6.02577	C39	–0.02805	6.02805
C10	–0.02805	6.02805	C40	–0.02577	6.02577
C11	–0.17573	6.17573	C41	–0.17678	6.17678
H12	0.21625	0.78375	H42	0.21364	0.78636
C13	–0.18444	6.18444	C43	–0.18358	6.18358
C14	–0.18358	6.18358	C44	–0.18444	6.18444

Cont…

C15	–0.17678	6.17678	C45	–0.17573	6.17573
H16	0.20492	0.79508	H46	0.20488	0.79512
H17	0.20943	0.79057	H47	0.21097	0.78903
H18	0.21097	0.78903	H48	0.20943	0.79057
H19	0.20488	0.79512	H49	0.20492	0.79508
H20	0.20506	0.79494	H50	0.20446	0.79554
H21	0.20446	0.79554	H51	0.20506	0.79494
H22	0.21364	0.78636	H52	0.21625	0.78357
C23	0.81828	5.18172	C53	0.84711	5.15289
O24	–0.57942	8.57942	O54	–0.65825	8.65825
O25	–0.68221	8.68221	O55	–0.67461	8.67461
H26	0.47829	0.52171	H56	0.50596	0.49404
C27	0.84710	5.15290	C57	0.81828	5.18172
O28	–0.65825	8.65825	O58	–0.57942	8.57942
O29	–0.67462	8.67462	O59	–0.68221	8.68221
H30	0.50596	0.49404	H60	0.47829	0.52171

Table 6. Donor, acceptor and stabilization energies for dimer structure of 9,10-Anthracenedicarboylic acid.

Donor (i)	Occupancy	Acceptor (j)	Occupancy	$E^{(2)}$ kcal/mol	E(j)-E(i) (au)	F(i,j) (au)
n_1 O28	1.95853	σ*O55-H56	0.06623	7.65	1.07	0.081
n_2 O28	1.84771	σ*O55-H56		19.37	0.70	0.107
n_1 O54	1.95853	σ*O29-H30	0.06624	7.65	1.07	0.081
n_2 O54	1.84771	σ*O29-H30		19.37	0.70	0.107

Table 7. Orbital occupancies, polarization coefficients, NBO description and contribution of *s* character for dimer of 9,10-Anthracenedicarboxylic acid.

NBOs Ω/ Ω* (A-B)	Occupancy q	C_A^2	C_B^2	Description of NBOs	s character (%) A	B
σ (C8-C27)	1.97122	51.54	48.46	$0.7179(sp^{2.53})C_8 + 0.6961(sp^{1.58})C_{27}$	28.27	38.74
σ*(C8-C27)	0.06125	48.46	51.54	$0.6961(sp^{2.53})C_8 + 0.7179(sp^{1.58})C_{27}$		
σ (C27-O28)	1.99402	33.54	66.46	$0.5791(sp^{2.26})C_{27} + 0.8152(sp^{1.61})O_{28}$	30.60	38.33
σ*(C27-O28)	0.04136	66.46	33.54	$0.8152(sp^{2.26})C_{27} + 0.5791(sp^{1.61})O_{28}$		
σ (C27-O29)	1.99491	32.22	67.78	$0.5676(sp^{2.52})C_{27} + 0.8233(sp^{1.82})O_{29}$	28.31	35.37
σ*(C27-O29)	0.07794	67.78	32.22	$0.8233(sp^{2.52})C_{27} + 0.5676(sp^{1.82})O_{29}$		
σ (O29-H30)	1.98327	78.03	21.97	$0.8833(sp^{3.02})O_{29} + 0.4687(sp^{0.00})H_{30}$	24.87	99.76
σ*(O29-H30)	0.06624	21.97	78.03	$0.4687(sp^{3.02})O_{29} + 0.8833(sp^{0.00})H_{30}$		
n_1 O28	1.95853			$sp^{0.81}$	55.28	
n_2 O28	1.84771			$sp^{26.47}$	3.64	

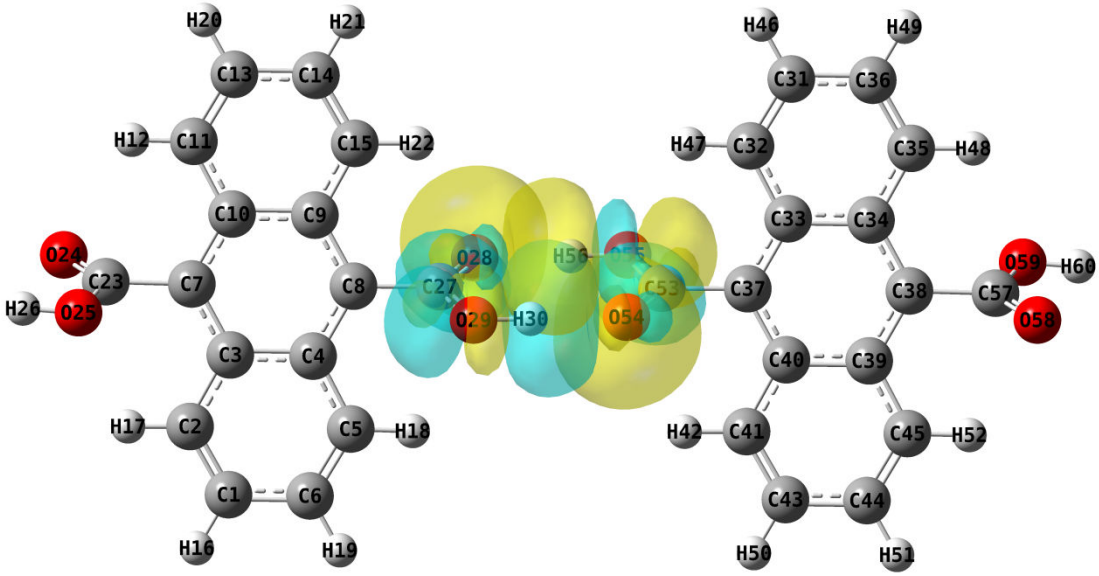

(a). Lone pair 1 n(O28)→ σ*(O55-H56)
and n(O54)→ σ*(O29-H30)

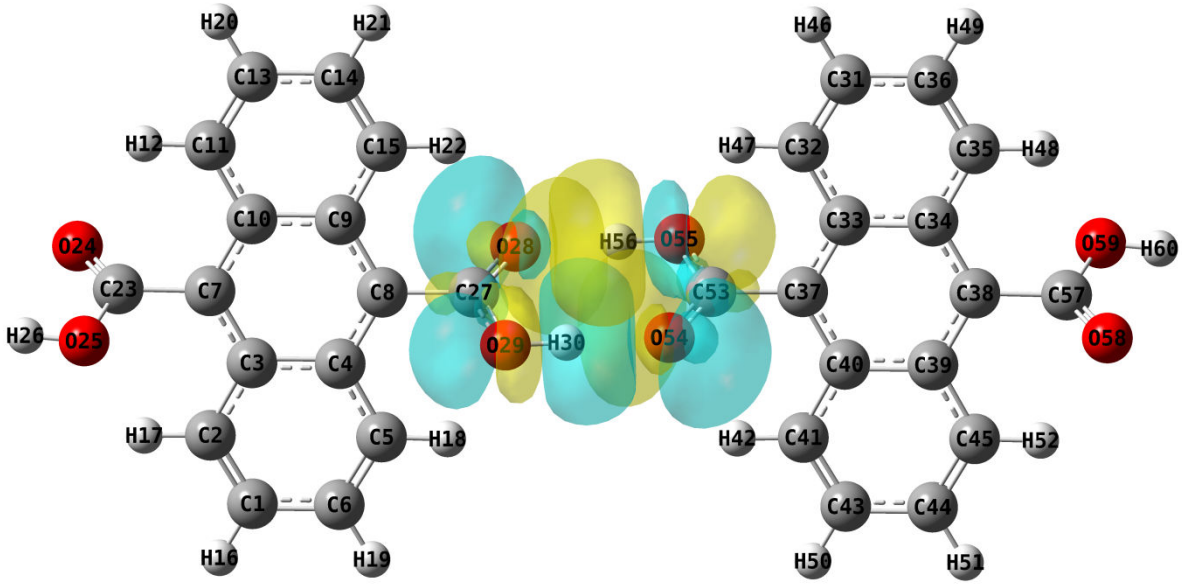

(b). Lone pair 2 n(O28)→ σ*(O55-H56)
and n(O54)→ σ*(O29-H30)

Figure 9. Electron density maps showing orbital overlaps in O─H•••O bonds of dimer structure: Donor (lone pairs 1 and 2 orbitals of O28 and O54) and Acceptor (anti-bonding orbitals of H56─O55 and H30─O29) are shown in (**a** and **b**).

4.5. AIM and NCI analysis

The investigations of molecular interactions by topological approaches such as quantum theory of atoms in molecules (QTAIM) and noncovalent interactions (NCI) analysis provides a deeper understanding of the interactions in terms of electron density, $\rho(\boldsymbol{r})$ and its Laplacian, $\nabla^2\rho(\boldsymbol{r})$. In QTAIM theory, these topological parameters evaluated at the bond critical points (BCPs) and ring critical points (RCPs) give the nature and the strengths of the interactions. Fig. 9 depicts the calculated molecular graph of D_{11} via QTAIM method. As can be seen, the topological structure exhibits a BCP and a bond path between the –C53=O54 and –O29─H30 groups and –C27=O28 and –O55─H56 groups; confirming the presence of two inter-molecular O─H•••O bonds in D_{11}. We have evaluated the strengths of these interactions as interaction energies using potential energy density, $V(\boldsymbol{r})$, at O•••H BCPs that are summarized in the Table 7. The $\rho(\boldsymbol{r})/\nabla^2\rho(\boldsymbol{r})$ values for inter-molecular O─H•••O bonds identified with BCP index 109 and 101 are calculated at 0.0450/0.1339 au and 0.0450/0.1339 au respectively. Each bond is characterized by interaction energy of 13.08 kcal/mol. The bonds are strong [27]. Additionally, the QTAIM analysis has provided the clear evidences for the presence of intra-molecular C─H•••O bonds in D_{11}. The BCP indices 75, 81, 114, and 123 associated with the C─H•••O bonds are characterized by 2.28-2.47 kcal/mol. We notice that the values of $\rho(\boldsymbol{r})$ and $\nabla^2\rho(\boldsymbol{r})$ for these indices are less than the corresponding values for O─H•••O bonds (see Table 5). In summary, the theoretically predicted topological parameters compared in the Table 5 suggest that O─H•••O bonds are stronger than C─H•••O bonds [28].

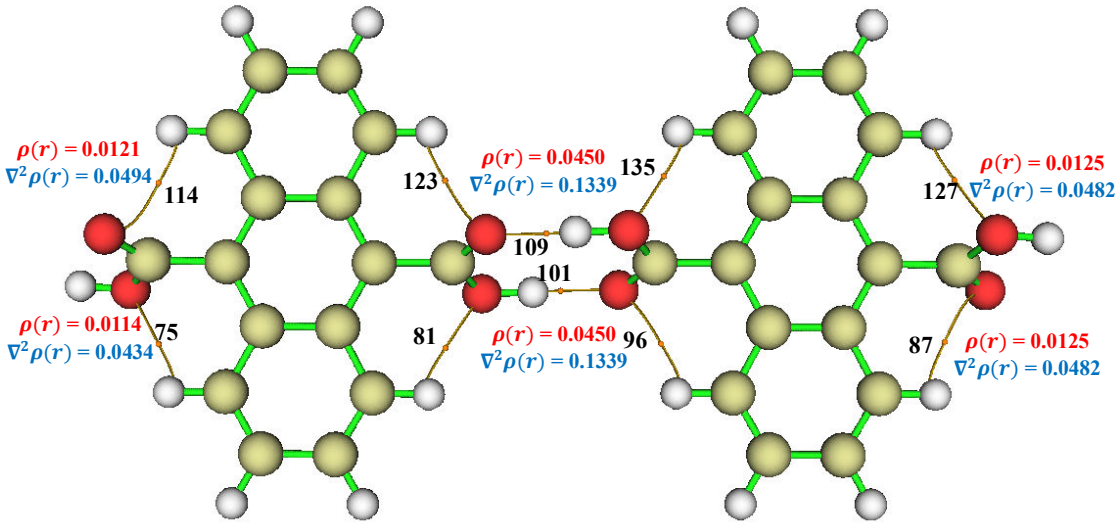

Figure 10. Bond Critical Point (BCP) indexes are 75, 114, 81, 123, 96, 135, 87, 127 (intra) and 109, 101 (inter) for dimer of 9,10-Anthracenedicarboxylic acid. The values of electron density (red) and its Laplacian (blue) correspond to the BCP indexes.

Table 8. Computed electron density, its Laplacian, potential energy density and interaction energies corresponding to BCP indexes of dimer structure.

Dimer BCP index	$\rho(\boldsymbol{r})$ **au**	$\nabla^2\rho(\boldsymbol{r})$ **au**	$V(\boldsymbol{r})$ **au**	$\boldsymbol{E_{HB}}$ **kcal/mol**
75 (intra)	0.0114	0.0434	–0.0073	2.28
114 (intra)	0.0121	0.0494	–0.0078	2.44
81 (intra)	0.0125	0.0482	–0.0079	2.47
123 (intra)	0.0125	0.0482	–0.0079	2.47
109 (inter)	0.0450	0.1339	–0.0417	13.08
101 (inter)	0.0450	0.1339	–0.0417	13.08

To analyze the H-bonding, *van der Waals* and steric repulsive interactions in the real space, we have performed the NCI analysis [29]. In particular, the NCI scatter graph and isosurfaces characterize the attractive and repulsive interactions by using blue-green-red (BGR) color code in which the blue region shows strong attractive interactions such as O─H•••O bonds, green-red region indicates the weak *van der Waals* and red region shows the strong repulsive steric interactions. In Fig. 10 we have shown the 2D scatter and 3D isosurfaces graphs for D_{11}. The scatter graph shows a low-gradient low-density spike at $sign(\lambda_2)\rho(r) = -0.014$ au, being characteristic of weak vdW interactions. The corresponding isosurface is green-red. The spike with low-gradient but high-density appeared at $sign(\lambda_2)\rho(r) = -0.0450$ au with blue isosurfaces between –C=O and –O─H groups is attributed to the inter-molecular O─H•••O bondings. The steric repulsive interactions in D_{11} have appeared as red isosurfaces. The spike in the 2D graph for these interactions has appeared at about $sign(\lambda_2)\rho(\mathbf{r}) = 0.02$ au The NCI analysis suggest that O─H•••O H-bonds are stronger than C─H•••O and weak van der Waals attractive interactions. Consequently, the elongation of O─H bond lengths has increased the vibrational anharmonicity of the modes resulting in red-shifted IR absorptions that are measured at 2896 & 2849 cm^{-1}.

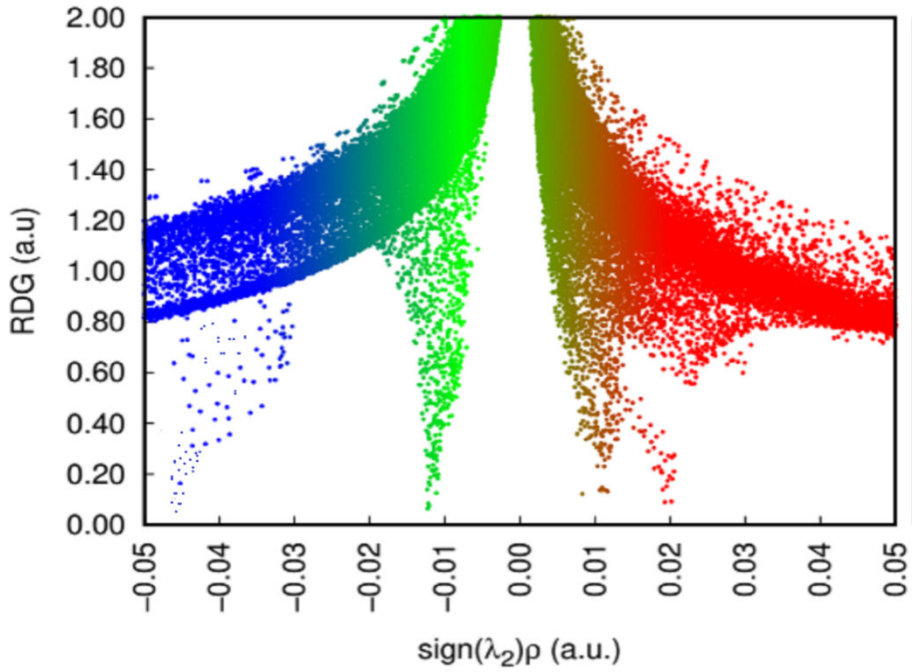

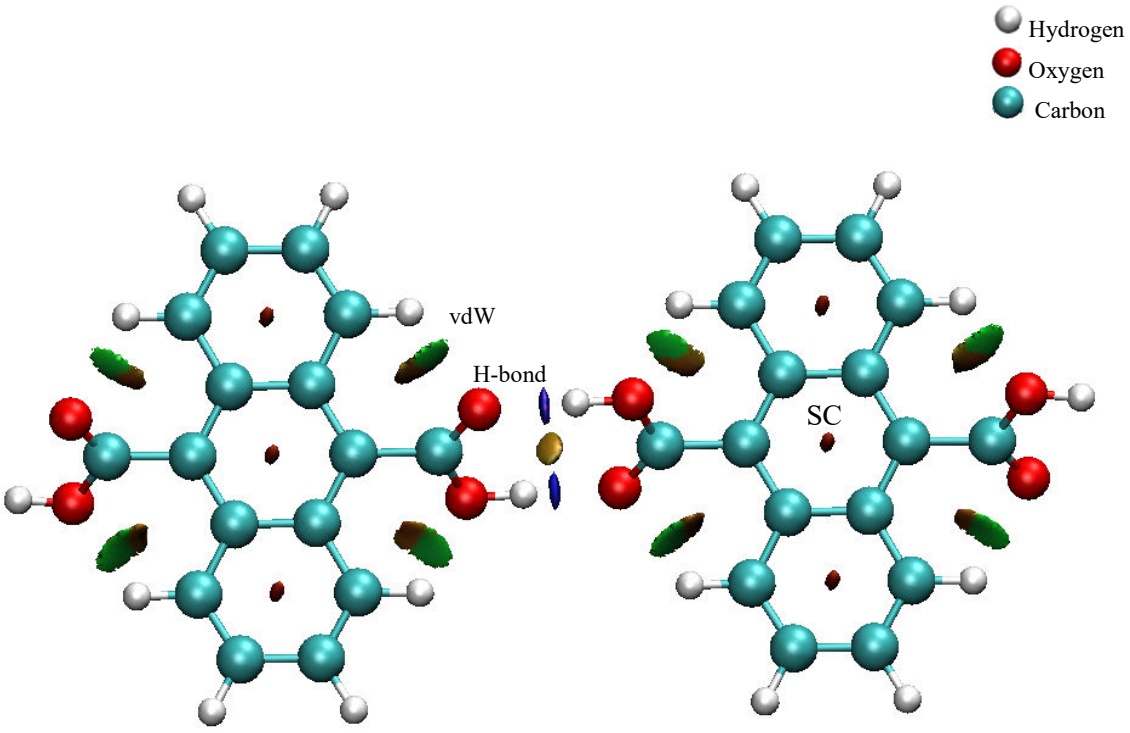

Figure 11. 2D scattered graphs for dimer, showing steric repulsion interaction when $\lambda_2>0$ and the *van der Waals* and H-bond interactions when $\lambda_2<0$. The gradient isosurfaces shown correspond to 2D scattered graphs.

5. CONCLUSIONS

The experimental FT-IR and FT-Raman spectral features of the organic linker 9,10-Anthracenedicarboxylic acid have shown O─H•••O H-bonding between the carboxylic groups of two monomeric units. Moreover, the H-bonded species are found to be cyclic-type as the bands due to –C=O stretch are mutually exclusive; IR active band at 1685 cm^{-1} and Raman active band at 1632 cm^{-1}. Accordingly, DFT cyclic-dimer model at the B3LYP/6-311++G(d,p) level has been proposed to account for the H-bond-induced modified vibrational structure. The vibrational spectrum of cyclic-dimer, D_{11}, constructed out of the most stable monomer, M_1, is in very good agreement with the experiment. The broad absorption in the 2500 - 3100 cm^{-1} region with two maxima at 2896 and 2849 cm^{-1} due to O─H•••O bonded –O─H stretch are calculated fairly accurately at 2896 and 2849 cm^{-1}. IR absorption at 1685 cm^{-1} and Raman line at 1632 cm^{-1} assigned to –C=O stretch are calculated at 1673 and 1652 cm^{-1} respectively. The H-bond protons resonances measured at 14.19 ppm in the ^1H NMR spectrum recorded in d_6-DMSO solvent has been accurately calculated at 14.4 ppm. The analysis of natural charges, orbital overlap and stabilization energies by NBO method and the topological parameters such as electron density, $\rho(\boldsymbol{r})$ and its Laplacian, $\nabla^2\rho(\boldsymbol{r})$ at H•••O BCPs as calculated by AIM method suggest that inter-molecular O─H•••O bonds are strong and linear. Additionally, the NCI analysis has provided the spatial representation of attractive (H-bonding and *van der Waals*) and repulsive (steric clashes) sites in D_{11} in terms of 2D scatter and 3D isosurface plots. We conclude that all the results point to the presence of the cyclic-O─H•••O dimer as a basic structural unit for the organic linker 9,10-Anthracenedicarboxylic acid characterized with consistent structural, vibrational and electronic properties and some of them in agreement with experiment.

References

[1] Jun-Jie Wang, ZeChang, Tong-Liang Hu, *Cadmium (II) and lanthanum (III) coordination architectures with anthracene-9,10-dicarboxylate: Crystal structures and photoluminescent properties,* Inorganica Chimica Acta. 385 (**2012**) 58-64.

[2] Jun-Jie Wang, Chun-Sen Liu, Tong-Liang Hu, Ze Chang, Cai-Yun Li, Li-Fen Yan, Pei-Quan Chen, Xian-He Bu, Qiang Wu, Li-Juan Zhao, Zhe Wang and Xin-Zheng Zhang, *Zinc (II) coordination architectures with two bulky anthracene-based carboxylic ligands: crystal structures and luminescent properties,* Cryst Eng Comm. 10 (**2008**) 681-692.

[3] Chun-Sen Liu, E. Carolina Sañudo, Jun-Jie Wang, Ze Chang, Li-Fen Yan and Xian-He Bu, *Manganese (II) complexes with a bulky anthracene-based dicarboxylic ligand: Syntheses, crystal structures, and magnetic properties,* Austr. J Chem, 61 (**2008**) 382-390.

[4] Shengqian Ma, Xi-Sen Wang, Christopher D. Collier, Erika S. Manis, and Hong-Cai Zhou, *Ultramicroporous Metal- Organic Framework Based on 9, 10-Anthracene dicarboxylate for Selective Gas Adsorption*, Inorg. Chem. 46 (**2007**) 8499-8501.

[5] Shengqian Ma, Jason M. Simmons, Daqiang Yuan, Jian-Rong Li, Wei Weng, Di-Jia Liua and Hong-Cai Zhou, *A nanotubular metal-organic framework with permanent porosity: structure analysis and gas sorption studies,* Chem. Comm. 385 (**2009**) 4049-4051.

[6] Heinz Prof. Dr. Langhals, Gertrud Schönmann, *New anthracene dicarboxylic acid imide compounds useful e.g. as photodimerisation product for treating tumors, vat dye, dihydroanthercenebisimde compound and bisanthracene dicarboxylic acid imide compounds,* Bundesrepublik Deutschland Deutsches Patent. 19 (**2007**) 1-59.

[7] Rene More, Gerhard Busse, Jorg Hallmann, Carsten Paulmann, Mirko Scholz and Simone Techert, *Photodimerization of Crystalline 9-Anthracenecarboxylic Acid: A Nontopotactic Autocatalytic Transformation,* J. Phys. Chem. C. 114 (**2010**) 4142–4148.

[8] Saisai Chen, Shengbao Xiao, Jin Liu & Zhen Li, *Synthesis and hydrogen storage properties of zirconium metal-organic frameworks UIO-66(H2ADC) with 9,10-anthracenedicarboxylic acid as ligand,* J. Por. Mat. 25 (**2018**) 1783–1788.

[9] Lingyan Zhu, Rabih O. Al-Kaysi, Robert J. Dillon, Fook S. Tham, and Christopher J. Bardeen, *Crystal Structures and Photophysical Properties of 9-Anthracene Carboxylic Acid Derivatives for Photomechanical Applications,* Am. Chem. Soc. 11 (**2011**) 4975–4983.

[10] Jun-Jie Wang, Dao-Jun Zhang, Ren-Chun Zhang, Xiao-Li Lu, Er-Ni Wang, Feng Jin& Yun-Feng Shi, *Syntheses, crystal structures and properties of complexes with two anthracene-based bulky backbone ligands,* Tran. Met. Chem. 40 (**2015**) 69–77.

[11] Muhammad Safdar, Amr Ghazy, Minnea Tuomisto, Mika Lastusaari & Maarit Karppinen, *Effect of carbon backbone on luminescence properties of Eu-organic hybrid thin films prepared by ALD/MLD* J. Mat. Sci. 56 (**2021**) 12634–12642.

[12] Jennifer M, Rowe Jennifer M, Hay William A, Maza Robert C, Chapleski Jr Erin Soderstrom Diego Troya Amanda J. Morris, *Systematic Investigation of the Excited-State Properties of Anthracene-Dicarboxylic Acids,* J. Photoche. and Photobio A: Chem. 6030 (**2016**) 30802-4.

[13] Lawrence j. Fitzgerald and roger e. Gerkin, *Anthracene-9-carboxylic Acid,* Acta Cryst. C53 (**1997**) 71-73.

[14] F. Bardak, C. Karaca, A. Atac, T. Mavis, A.M. Asiri, M. Karabacak, E. Kose, *Conformational, electronic, and spectroscopic characterization of Isophthalic acid (monomer and dimer structures) experimentally and by DFT,* Spectrochimica Acta Part A: Mol. and Bio. Spec. 165 (**2016**) 33-46.

[15] G.R. Desiraju, T. Steiner, *The Weak Hydrogen Bond: In Structural Chemistry and Biology,* Oxford University Press, **2001**.

[16] N. Sundaraganesan, S. Ilakiamani, H. Saleem, P. M. Wojciechowski, D. Michalska, *FT-Raman and FT-IR spectra, vibrational assignments and density functional studies of 5-bromo-2-nitropyridine,* Spectrochimica Acta Part A: Mol. and Bio. Spec. 61 (**2005**) 2995–3001.

[17] V. Krishnakumar, R. Ramasamy, *Scaled quantum chemical studies of the structure and vibrational spectra of 2-(methylthio) benzimidazole,* Spectrochimica Acta Part A: Mol. and Bio. Spec. 62 (**2005**) 570-577.

[18] M. Silverstein, G. C. Basseler, C. Morill, *Spectrometric Identification of Organic Compounds,* Wiley, New York, **1981**.

[19] G. Varsanyi, *Assignments of Vibrational Spectra of 700 Benzene Derivatives,*Wiley, New York, **1974**.

[20] Y.X. Sun, Q.L. Hao, Z.X. Yu, W.J. Jiang, L.D. Lu, X. Wang,*Experimental and theoretical studies on vibrational spectra of 4-(2-furanyl methylene amino) antipyrine, 4benzylidene amino antipyrine and 4cinnamilidene amino antipyrine,* Spectrochimica Acta Part A: Mol. and Bio. Spec. 73 (**2009**) 892-901.

[21] A. Altun, K.Gölcük, M.Kumru, *Structure and vibrational spectra of p-methylaniline: Hartree-Fock, MP2 and density functional theory studies,* J. Mol. Stru. 637 (**2003**) 155-169.

[22] Norman B. Colthup, L.H. Daly, S.E. Wiberley, *Introduction to Infrared and Raman Spectroscopy,* Academic Academic Press, New York and London, **1964**.

[23] Mehmet Karabacak, Mehmet Cinar, Zeliha Unal, Mustafa Kurt, *FT-IR, UV spectroscopic and DFT guantum chemical study on the molecular conformation, vibrational and electronic transitions of 2-aminoterephthalic acid,* J. Mol. Stru. 982 (**2010**) 22-27.

[24] Ramanna P, Jayashree Tonannavar, J. Tonannavar, *Study of H-bonded cyclic dimer of organic linker 5-Bromoisophthalic acid by DFT and vibrational spectroscopy,* J. Mol. Stru. 1241 (**2021**) 130613.

[25] RA Yadav, IS Singh, *Intermolecular hydrogen-bonding in o-ethyl and m-ethyl phenols,* J. Pure Appl. Phys.23 (**1985**) 626-627.

[26] N. Sundaraganesan B. Anand C. Meganathan B. Dominic Joshua H. Saleem, *Vibrational spectra and assignments of 3-aminobenzyl alcohol by ab initio Hartree–Fock and density functional method,* Spectrochimica Acta Part A: Mol. and Bio. Spec. 69 (**2008**) 198-204.

[27] I. Rozas, I. Alkorta, J. Elguero, *Behavior of Ylides Containing N, O, and C Atoms as Hydrogen Bond Acceptors* J. Am. Chem. Soc. 122 (**2000**) 11154-11161.

[28] Shivanand S. Malaganvi, J. Tonannavar Yenagi, J. Tonannavar, *Spectroscopic and electronic structure characterization of hydrogen bonding in 2-Bromohydroquinone,* J. Mol. Stru. 1181 (**2019**) 71-82.

[29] E.R. Johnson, S. Keinan, P. Mori-Sanchez, J. Contreras-Garcia, A.J. Cohen, W. yang, *Revealing non-covalent interactions,* J. Am. Chem. Soc. 132 (**2010**) 6498–6506.